

Supplementary Information

In-situ spectroscopy on (Pt(acac)₂) decomposition at sub-second time resolution.

Jakub Szlachetko^{*1,2}, Maarten Nachtegaal^{*1}, Jacinto Sá¹, Jean-Claude Dousse³, Joanna Hoszowska³, Evgeny Kleymenov^{1,4}, Markus Janousch¹, Olga V. Safonova¹ and Jeroen A. van Bokhoven^{*1,4}

Generalized Kramers-Heisenberg formula.

Based on the formulas developed by Tulkki and Åberg (1, 2) within the Kramers-Heisenberg approach, the differential cross sections for resonant X-ray scattering can be expressed as follows:

$$\frac{d\sigma(\omega_1)}{d\omega_2} \approx 2\pi r_0^2 \int \frac{\omega_2}{\omega_1} \frac{(\omega_{initial} - \omega_{final}) g_{final \rightarrow initial} (\omega_{initial} + \omega) \cdot \frac{dg_{initial}}{d\omega}}{(\omega_{initial} + \omega - \omega_1)^2 + \Gamma_{initial}^2 / 4\hbar^2} \times \frac{\Gamma_{final} / 2\hbar}{(\omega_1 - \omega_{final} - \omega - \omega_2)^2 + \Gamma_{final}^2 / 4\hbar^2} d\omega \quad (1)$$

where r_0^2 is the classical electron radius. The energies of the initial and final states are represented by $\hbar\omega_{initial}$ and $\hbar\omega_{final}$, whereas $\hbar\omega_1$ and $\hbar\omega_2$ are the incoming and outgoing photon energies, respectively. The initial and final state broadening are given by $\Gamma_{initial}$ and Γ_{final} . The $g_{final \rightarrow initial}$ stands for the oscillator strength of the X-ray transition from the final to initial vacancy state, and the $dg_{initial}/d\omega$ represents the oscillator strength distribution for electron excitation.

To account for the incoming beam energy distribution ($dN_{beam}/d\omega_1$) and the resolution of the X-ray detector ($dN_{detector}/d\omega_2$), the measured differential cross sections can be written as:

$$\frac{d\sigma_{measured}(\omega_1)}{d\omega_2} \approx \int \int \frac{d\sigma(\omega_1)}{d\omega_2} \cdot \frac{dN_{beam}}{d\omega_1} \cdot \frac{dN_{detector}}{d\omega_2} d\omega_1 d\omega_2 \quad (2)$$

The second term in equation (1) ensures the energy conservation given by $\omega = \omega_1 - \omega_{final} - \omega_2$ and accounts for the final state broadening (Γ_{final}). By neglecting the final state width the second term of Eq.1 can be replaced by the Dirac delta function (1, 2):

$$\frac{d\sigma(\omega_1)}{d\omega_2} \approx 2\pi r_0^2 \int \frac{\omega_2}{\omega_1} \frac{(\omega_{initial} - \omega_{final}) g_{final \rightarrow initial} (\omega_{initial} + \omega) \cdot \frac{dg_{initial}}{d\omega}}{(\omega_{initial} + \omega - \omega_1)^2 + \Gamma_{initial}^2 / 4\hbar^2} \delta(\omega_1 - \omega_{final} - \omega - \omega_2) d\omega \quad (3)$$

In our study, we demonstrated that for the off-resonant excitations the oscillator strength distribution ($dg_{initial}/d\omega$) is directly proportional to the X-ray absorption spectrum (XAS). Therefore, the shape of the X-ray emission spectrum (XES), which is comparable to the differential cross sections, can be described as follows:

$$XES(E_2) \approx \int \frac{E_2}{E_1} \frac{(E_{initial} - E_{final})(E_{initial} + E) \cdot XAS(E)}{(E_{initial} + E - E_1)^2 + \Gamma_{initial}^2 / 4} \delta(E_1 - E_{final} - E - E_2) dE \quad (4)$$

In the above equation the constants were omitted and frequencies replaced by E according to $\omega = E/\hbar$. This simplified formula provides the XAS(E) function that can be numerically solved for any measured XES(E₂). The final state broadening (Γ_{final}), the incoming beam energy distribution ($dN_{beam}/d\omega_1$) and the resolution of the X-ray detector ($dN_{detector}/d\omega_2$) are not considered in this equation. Therefore the derived XAS curves will be broadened by these three contributions. In the calculations, the energies of the initial and final states were taken from (3) and the width of the initial state from (4).

In order to compare the reconstructed XAS(E) to measured conventional XAS, additional core-hole lifetime broadening was introduced. The results of the convolution are presented in Fig.1 for different life-time broadening. As shown, the best agreement was obtained for a Lorentz width of 4.8eV that is very close to the natural lifetime broadening of 5.4eV (4) for the Pt L₃ state. The small discrepancy can be accounted for by the spectrometer broadening that is included in the measured XAS(E) spectrum.

Experiment details

The HEROS experiments were performed at the SuperXAS beamline of the Swiss Light Source at the Paul Scherrer Institute, Switzerland. The X-ray beam delivered by the 2.9 Tesla super-cooled bending magnet was collimated by a spherically bent Rh mirror. The collimated X-rays were monochromatized by means of a double Si(111) crystal monochromator and focused by a toroidally bent Rh mirror. On the sample the photon flux was $7-8 \times 10^{11}$ photons/sec with an energy resolution of $\Delta E/E \approx 1.4 \times 10^{-4}$ and a spot size of $100 \mu\text{m}^2$. For calibration a 4 μm thick Pt foil was used. The Pt TFY-XAS spectra were recorded with the same experimental setup by scanning the incident beam energy across the absorption edge. The TFY-XAS spectrum was constructed from the total integrated intensity of the L_{α1} fluorescence.

For X-ray detection a wavelength-dispersive spectrometer was adapted. To avoid any scanning components during the acquisition, the spectrometer was operated in the von Hamos geometry. The X-rays emitted from the sample were diffracted by a Ge(660) crystal bent cylindrically to a radius of curvature of 25.4cm. The crystal size was 10cm and 5cm in the focusing and dispersive axes, respectively. For the detection of the diffracted photons, a 1D-array, single photon counting, MythenII was employed. The spectrometer was operated in the vertical scattering geometry.

The experimental response of the spectrometer, which was determined from the measurements of the Rayleigh scattering, was found to be well reproduced by a Gaussian function. Full width at half maximum experimental broadenings Γ_{exp} of 1.7eV was obtained. The achieved resolution was far below the natural width (Γ_{initial}) of the $L_{2p3/2}$ core-hole (5.39 eV for Pt) (4). The energy calibration of the spectrometer and of the beam energies was based on the measurements of the $La_{1,2}$ fluorescence and Rayleigh scattering. The tabulated values of the transition energies were used (3). The stability of the setup was controlled constantly during the experiment and no significant deviations were observed neither in the energy calibration nor in the measured intensity.

References

1. J. Tulkki and T. Åberg, *J. Phys. B* **15**, L435 (1982).
2. T. Åberg and J. Tulkki, *Plenum Press, New York*, Atomic Inner-Shell Physics 419–463 (1985).
3. R. D. Deslattes, E. G. Kessler, *Rev. Mod. Phys.* **75**, 35 (2003).
4. J. L. Campbell, T. Papp, *Atom. Data Nucl. Data Tables* **77**, 50 (2001).

Figures:

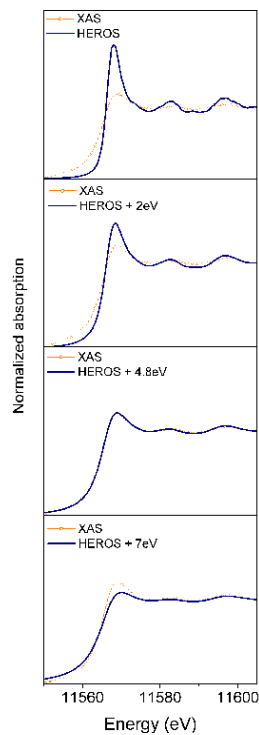


Figure 1: Result of the convolution of the HEROS spectra with a Lorentz function with different full widths at half maximum. As shown, the best agreement between reconstructed and conventional XAS is obtained for a FWHM of 4.8eV